Journal of Hydrology (2007) 340, 48–62

available at www.sciencedirect.com

ScienceDirect

journal homepage: www.elsevier.com/locate/jhydrol

Field-derived relationships for flow velocity and resistance in high-gradient streams

Francesco Comiti [a,*], Luca Mao [a], Andrew Wilcox [b,c], Ellen E. Wohl [c], Mario A. Lenzi [a]

[a] *Department of Land and Agro-Forest Environments, University of Padova, Agripolis, viale dell'Università 16, 35020 Legnaro (PD), Italy*
[b] *US Geological Survey, Geomorphology and Sediment Transport Laboratory, 4620 Technology Drive, Suite 400, Golden, CO 80403, USA*
[c] *Department of Geosciences, Colorado State University, Fort Collins, CO 80523-1482, USA*

Received 29 September 2006; received in revised form 9 March 2007; accepted 31 March 2007

KEYWORDS
Step-pool;
Flow resistance;
Steep channels;
Salt tracers;
Mountain rivers

Summary We measured velocity and channel geometry in 10 reaches (bed gradient = 0.08—0.21) of a predominantly step-pool channel, the Rio Cordon, Italy, over a range of discharges (3—80% of the bankfull discharge). The resulting data were used to compute flow resistance. At-a-station hydraulic geometry relations indicate that in most reaches, the exponent describing the rate of velocity increases with discharge was between 0.48 and 0.6, which is within the range of published values for pool-riffle channels. The Rio Cordon data are also combined with published hydraulics data from step-pool streams to explore non-dimensional relationships between velocity and flow resistance and factors including unit discharge, channel gradient, and step geometry. Multiple regression analysis of this combined field dataset indicated that dimensionless unit discharge (q^*) is the most important independent variable overall in explaining variations in velocity and flow resistance, followed by channel slope and the ratio of step height to step length. Empirical equations are provided both for dimensionless velocity and flow resistance, but prediction of the former variable appears more reliable.

Introduction

Resolving the substantial uncertainties surrounding the evaluation of flow resistance, the mechanics of sediment transport and the dynamics of channel form is needed to advance understanding of physical processes in steep

* Corresponding author. Tel.: +39 049 8272695; fax: +39 049 8272686.
E-mail address: francesco.comiti@unipd.it (F. Comiti).

0022-1694/$ - see front matter © 2007 Elsevier B.V. All rights reserved.
doi:10.1016/j.jhydrol.2007.03.021

(>3–5%) mountain streams (Lenzi et al., 2004, 2006a; Chin and Wohl, 2005). Quantification of flow velocity is important both for engineering problems (e.g., determination of flood hydrographs, water levels and sediment transport) and for ecological assessments (e.g., habitat or pollutant dispersion modeling). Methods of predicting flow velocity in steep channels using reliable, easily measurable channel characteristics are therefore needed for a range of applications.

Hydraulically rough flows in high-gradient streams have been investigated for decades (e.g., Peterson and Mohanty, 1960; Judd and Peterson, 1969), although many such studies have been carried out using simplified flume modelling of the complex bed morphology that often characterizes steep channels. These channels typically have step-pool and cascade morphologies (Montgomery and Buffington, 1997; Wohl, 2000) that feature a ''tumbling flow'' pattern (Peterson and Mohanty, 1960) characterized by pseudo-cyclic acceleration and deceleration. In step-pool channels, supercritical flow ($Fr > 1$) typically occurs from the step lip to the impingement point, whereas sub-critical ($Fr < 1$) conditions establish thereafter in the pool, with the change occurring via a hydraulic jump (Wohl and Thompson, 2000; Wilcox and Wohl, 2006a; Valle and Pasternack, 2006). The extent to which this alternation between super- and sub-critical flow persists at high to extreme flows is uncertain, however, when steps may eventually be drowned out or mobilized (Curran and Wilcock, 2005; Comiti et al., 2005; Comiti and Lenzi, 2006). Hydraulics in channels having step-pool and/or cascade morphology differ substantially from lower-gradient rivers as a result of the spill resistance generated by tumbling flow and hydraulic jumps, which dominates total flow resistance (Curran and Wohl, 2003; MacFarlane and Wohl, 2003; Wilcox et al., 2006). Therefore, existing equations for estimating flow resistance or sediment transport in lower-gradient channels, where grain roughness is often assumed to be the major component of flow resistance, have substantial error when applied to step-pool and other steep channels (Bathurst, 1985; Marcus et al., 1992; Millar, 1999; Curran and Wohl, 2003; MacFarlane and Wohl, 2003). As discussed in the next section, to our knowledge only one resistance equation based on field data has been derived for step-pool channels.

At-a-station hydraulic geometry provides another mechanism for evaluating the effect of roughness within a channel because of the interrelations among velocity, stage, roughness, and discharge. Leopold and Maddock's (1953) original development of at-a-station hydraulic geometry proposed that the relation of discharge to other hydraulic factors in natural river cross-sections can be described by the power functions, $w = aQ^b$, $d = cQ^f$, and $v = kQ^m$, where Q is discharge; w,d, and v represent water-surface width, mean depth, and velocity, respectively; a, c, and k are coefficients whose product is one; and b, f, and m are exponents that sum to one. Leopold and Maddock (1953) found that the relative rates of increase of width and depth are functions of channel shape, whereas the rate of increase of velocity reflects roughness of the channel boundaries. Subsequent investigators have used at-a-station hydraulic geometry relations to further explore the relations among channel shape, roughness, and hydraulic parameters (e.g. Richards, 1973; Knighton, 1975; Ferguson, 1986), although these inquiries have largely been restricted to pool-riffle channels. Limited data are available on hydraulic geometry relations in step-pool channels. In these channels, where relative submergence of bed materials is low, width-depth ratios are low, and hydraulics change substantially with discharge (e.g., Lee and Ferguson, 2002; Wilcox and Wohl, 2006a), relationships among velocity, discharge, and flow resistance may differ from those in lower-gradient channels.

In this paper, we explore factors influencing velocity and flow resistance in high-gradient channels in order to develop predictive equations for these hydraulic variables. First, we review previously developed equations for velocity and flow resistance in steep channels, all of which are entirely or primarily based on laboratory flume results. We then present new field data on velocity, flow resistance, and channel morphology over a range of discharges from a set of reaches in a predominantly step-pool stream in the Italian Alps. Linkages among velocity, flow resistance, and discharge in this channel are described in terms of at-a-station hydraulic geometry relations. Next, these data are combined with other, previously collected field datasets from step-pool channels to investigate relationships among both velocity and flow resistance and water discharge, channel slope, and bedform geometry. Field data are also compared to flume-based predictive relationships for steep channels. Because many of these analyses investigate relationships between velocity and unit discharge, they are most applicable to the prediction of velocity and flow resistance when water discharge is known or assumed, as is the case in many engineering or modelling applications, and unit discharge can be easily derived using measurements of channel width.

Velocity and resistance equations for step-pool systems

Flow resistance in closed conduits as well as in open-channel flows is commonly analyzed in terms of the Darcy–Weisbach friction factor, ff, defined as:

$$ff = \frac{8gR_h S}{v^2}. \quad (1)$$

where g is the acceleration due to gravity (m s^{-2}), R_h is the hydraulic radius (m), S is channel slope (m m^{-1}), and v is flow velocity (m s^{-1}).

Several authors have proposed resistance equations for step-pool channels. For example, Egashira and Ashida (1991) analytically developed a resistance formula for step-pool channels that they tested using flume studies. Their formula performed well only when steps were completely drowned out and no jumps occurred. When hydraulic jumps were present, the friction factor ff was found to be two to three times greater than that predicted by their equation.

Aberle and Smart (2003), using flume studies at slopes ranging from 0.02 to 0.098, produced the following resistance equation for steep channels:

$$\sqrt{\frac{8}{ff}} = 0.91\frac{d}{s}, \quad (2)$$

where d is mean flow depth (m) and s is the standard deviation of the bed profile, representing bed roughness. The combination of Eq. (2) with Eq. (1) and continuity give — assuming a rectangular cross-section — the following relationship expressed in terms of velocity (Aberle and Smart, 2003):

$$v = 0.96 g^{0.20} S^{0.20} q^{0.60} s^{-0.40}, \quad (3)$$

where q is discharge per unit width ($m^2 s^{-1}$). Rickenmann (1990, 1991) produced similar results, based on flume studies at slopes between 0.03 and 0.40:

$$v = 1.3 g^{0.20} S^{0.20} q^{0.60} D_{90}^{-0.40}, \quad (4)$$

where D_{90} is the 90th percentile of the bed grain size distribution (m) and is used instead of s to represent roughness.

Maxwell and Papanicolaou (2001) produced a roughness equation for step-pool channels, based on flume tests at slopes of 0.03—0.07, that incorporates the dimensions of step-pool features:

$$\sqrt{\frac{8}{ff}} = -3.73 \log\left(\frac{H \cdot D_{84}}{L \cdot d}\right) - 0.80, \quad (5)$$

where H is step height and L is step length (both in m).

The only resistance equation we are aware of that incorporates field data was published by Lee and Ferguson (2002), who measured mean velocity using salt-dilution methods in 6 step-pool reaches (S = 0.03—0.18) and in laboratory tests (S = 0.067) with self-formed alluvial steps:

$$\sqrt{\frac{8}{ff}} = 4.19\left(\frac{R_h}{D_{84}}\right)^{1.80}. \quad (6)$$

They recorded rapid increases in velocity as discharge increased, with correspondingly strong reductions in flow resistance. Lee and Ferguson also found that the Keulegan-type resistance formula proposed by Thompson and Campbell (1979) for stepped spillways was, among several published equations they tested, the most appropriate to use without any calibration.

Wilcox and Wohl (2006b) also examined controls on flow resistance in step-pool channels using flume experiments. They documented relationships between flow resistance and factors including LWD density and position on steps, step geometry, and slope, and they found that discharge strongly mediated the effects of bed roughness variables on flow resistance.

Methods

Study basin

Our field research was conducted in the Rio Cordon, a small stream (drainage area = 5 km^2) in the Dolomites, located in the Eastern Italian Alps (Fig. 1). The bedrock geology consists of dolomite, volcaniclastic conglomerates, and tuff sandstones. The main channel (0.136 mean gradient) features cascade and step-pool reaches, according to the Montgomery and Buffington (1997) classification. The mean diameter of the bed surface sediments along the main channel is 0.11 m, with a geometrical standard deviation $\sigma_g = (D_{84}/D_{16})^{0.5}$ = 3.12 (Mao, 2004). Clasts composing the bed

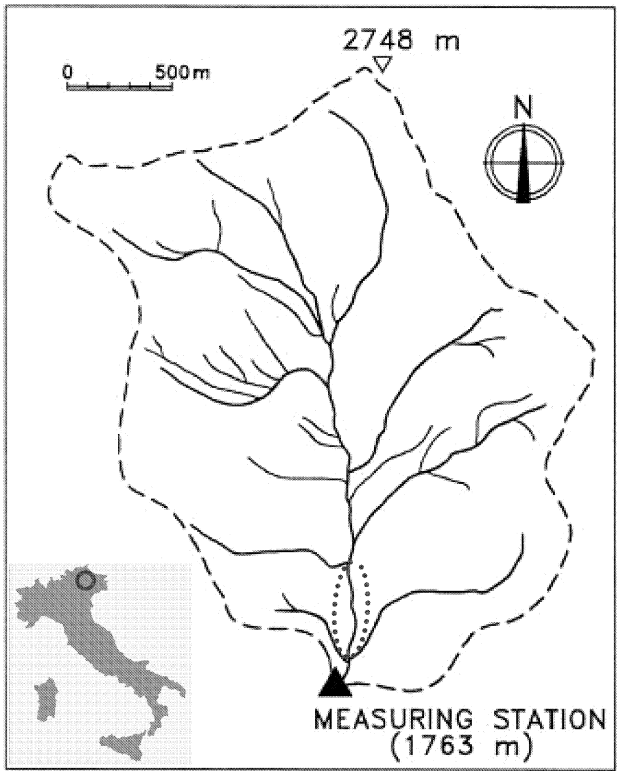

Figure 1 Location map of the Rio Cordon basin. The channel segment where measurements were carried out is marked.

alluvium are generally weakly rounded and poorly imbricated because the basin lithology supplies slab-like materials to the channel. The bankfull channel width varies from 5 to 6.7 m. The bankfull discharge, based on direct observation, is approximately 2.3 $m^3 s^{-1}$ (Lenzi et al., 2006a).

The basin hosts a long-term project for monitoring water and sediment fluxes, with an experimental facility operating since 1986. The instrumentation for measuring water discharge, suspended sediment, and bedload transport at the Rio Cordon experimental station has been described in detail in previous papers (Lenzi et al., 1999, 2004). Previous studies in the Rio Cordon have investigated the morphological structures of the stream bed (Lenzi, 2001), sediment yield and transport rates (Lenzi et al., 2003, 2004), incipient sediment motion (Lenzi, 2004, 2006b), size-selective and equal mobility transport conditions (Mao and Lenzi, 2007), determination of the effective discharge (Lenzi et al., 2006a), and linkages between three-dimensional hydraulics and channel morphology (Wilcox et al., 2006).

The climatic conditions of the basin are typical of an Alpine environment. Precipitation (annual average of about 1100 mm) occurs mainly as snowfall from November to April. Runoff is usually dominated by snowmelt in May and June, but summer and early autumn floods represent an important contribution to the flow regime.

Large woody debris (LWD) is practically absent in the Rio Cordon upstream of the experimental station, as a result of both natural and anthropogenic factors. Only 7% of the basin area, primarily the lower portion close to the measuring station, is forested. Moreover, occasional LWD inputs into the channel (eroding banks, natural tree falls, tributary debris

flows) have been removed for centuries by local people using the basin for cattle grazing and forest harvesting (Comiti et al., 2006).

Rio cordon field measurements and analysis

A detailed topographic survey along 600 m of channel upstream from the Rio Cordon experimental station was carried out in 2004 using a total station. Velocity measurements were performed in 10 reaches, the characteristics of which are described in Table 1, within this length of channel. Among these reaches, five (1A, 1B, 1C; 2A, 2B) consisted of shorter sub-reaches nested within longer reaches (1, 2), whereby reach-average velocities were measured for both the sub-reaches separately and the longer reaches as a whole. Most of the reaches can be classified as step-pool, with the exception of reaches 3 and 5, where cascade morphology dominates, and reach 1A, which has the lowest gradient and can be classified as a run (Figs. 2 and 3). Morphologic differences between reaches are subtle, however; cascade reaches are classified as such because pools are less developed than in step-pool reaches, and tumbling flow is less prevalent (but not absent) in the run reach (Figs. 2 and 3). Although the focus of this paper is on step-pool dynamics, the cascade and run reaches are included in subsequent analysis because of the subtle nature of transitions between morphologic types and, in some cases, as a point of comparison in hydraulics among different reaches.

The measurements of flow velocity were carried out using the salt dilution method (Calkins and Dunne, 1970). Portable conductivity meters (model WTW Cond340i with TetraCon 325 probes, storing data every 5 s) were placed at the upstream and downstream end of each study reach, and the distance and elevation change between the probes was surveyed as part of the longitudinal-profile surveys. As a tracer, a variable quantity (0.1–0.5 kg) of salt (NaCl) was mixed into a plastic bin filled with stream water, avoiding saturation. The salt mixture was then injected into the main stream at a distance of at least 10 channel widths upstream from the upper probe to promote adequate lateral mixing (Elder et al., 1991; D'Agostino, 2004). The time lag between the conductivity peaks recorded by the upstream and downstream instruments gives information on the average travel time of the flow, following the methods of Curran and Wohl (2003) and MacFarlane and Wohl (2003). The conductivity probes' acquisition step of 5 s makes this measure of the travel time susceptible to some error, especially in shorter reaches. Travel distance between the probes was divided by travel time to determine mean flow velocity.

Salt-tracer velocity measurements were repeated in each reach over a range of discharges, with at least three repetitions of salt injections performed in every reach for a single discharge. Overall, 44 pairs of discharge–velocity data were measured (averaged out of a total of 155 measurements) during snowmelt flows, summer low-flows and autumn high-flows, with a discharge range between 0.08 and 1.86 $m^3 s^{-1}$; i.e., approximately between 3% and 80% of the bankfull discharge.

Water discharge at the time of each velocity measurement was obtained from the downstream measuring station, which records discharge at 5-min intervals. The two small tributaries (Fig. 1) along the 600-m channel length between our uppermost study reach and the discharge measurement station are ephemeral and activate mostly during short, high-intensity rainfall. Therefore discharge data are assumed to be representative of all the surveyed reaches with a negligible (say <5%) error.

Three fixed cross-sections per reach were surveyed during each velocity measurement period. These sections were placed at intermediate locations between pools and steps, where the flow appeared to be closer to uniform conditions, and cross-sections with large boulders or other irregularities were also avoided. Channel geometry parameters (flow width w, wetted area A, wetted perimeter P, hydraulic radius R_h) were calculated using the software WinXSPRO 3.0 (Hardy et al., 2005).

We examined how velocity, width and flow depth change with discharge in the Rio Cordon using at-a-station hydraulic geometry analysis (Leopold and Maddock, 1953). Our analysis considered reach-average changes in hydraulics, using the reaches in Table 1, rather than changes at individual cross-sections. This approach obscures hydraulic differences between step lip, pool, and step tread portions of the channel but allows comparison between step-pool,

Table 1 Characteristics of the 10 reaches in the Rio Cordon, where S is channel slope, H is step height, L is step wavelength, s is standard deviation of the bed profile, D_{50} and D_{84} are 50th and 84th percentile of the grain size distribution respectively, σ_g is standard deviation of the grain size distribution

Reach	Morphology	Length (m)	S (m/m)	H/L (−)	$(H/L)/S$ (−)	s (m)	D_{50} (m)	D_{84} (m)	σ_g (−)
1	Step-pool	76.4	0.12	0.17	1.5	0.45	0.14	0.41	2.43
1A	Run	22.8	0.08	0.12	1.4	0.25	0.14	0.46	2.43
1B	Step-pool	16.1	0.18	0.27	1.4	0.36	0.15	0.33	2.43
1C	Step-pool	32.8	0.11	0.2	1.7	0.33	0.12	0.33	2.43
2	Step-pool	66.4	0.11	0.17	1.5	0.28	0.19	0.46	2.89
2A	Step-pool	29.4	0.10	0.18	1.9	0.25	0.20	0.51	2.89
2B	Step-pool	36.9	0.12	0.14	1.2	0.27	0.18	0.43	2.89
3	Cascade	38.5	0.14	0.18	1.4	0.29	0.22	0.48	3.04
4	Step-pool	42.0	0.14	0.17	1.2	0.37	0.15	0.47	3.54
5	Cascade	19.6	0.21	0.32	1.5	0.57	0.29	0.63	3.07

Reach 1 comprises three sub-reaches (1A, 1B, 1C) but extends for several meters upstream of the upper end of 1C, so that it is longer than the sum of the three sub-reaches. Reach 2 is exactly composed of its sub-reaches 2A and 2B.

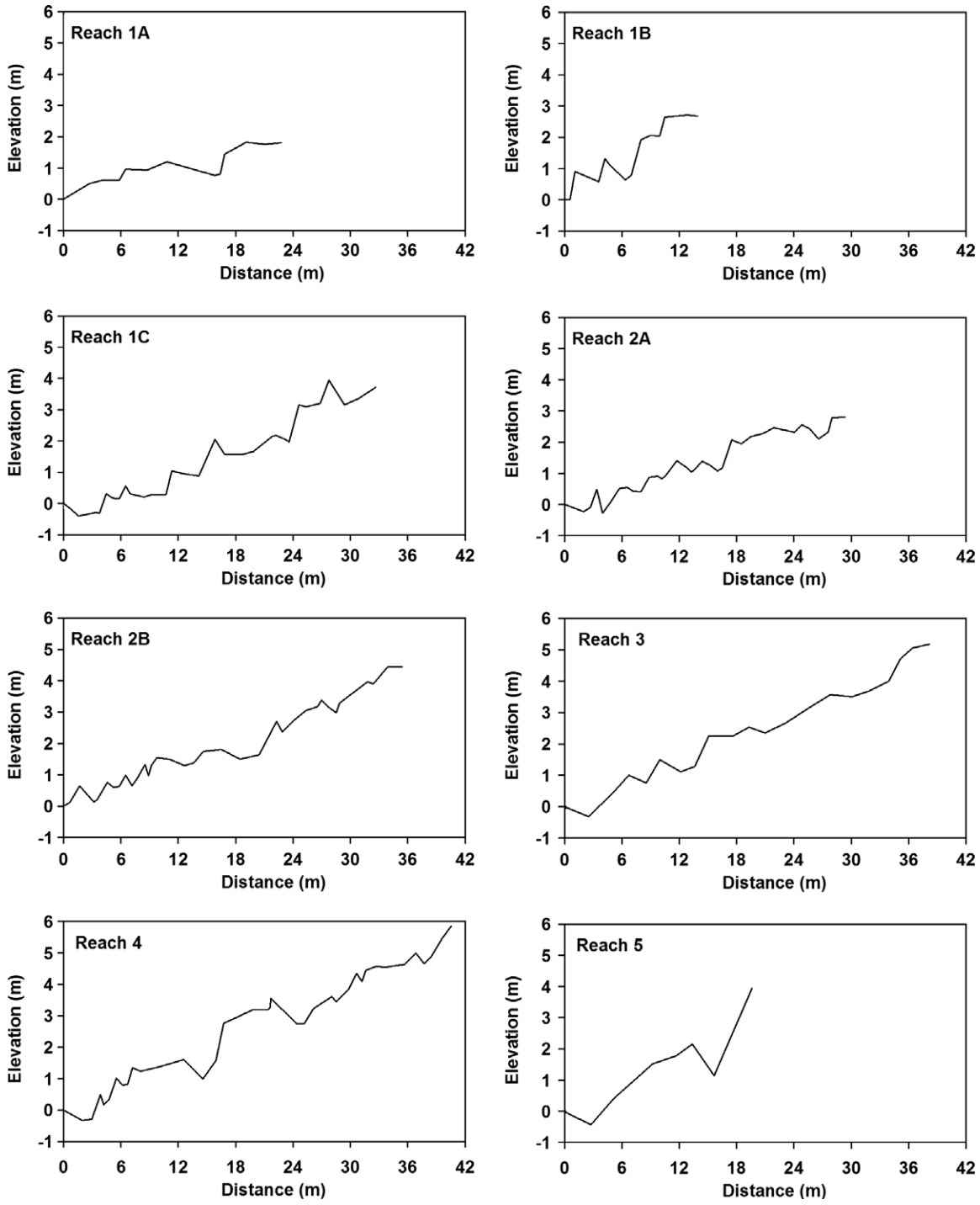

Figure 2 Longitudinal profiles of the reaches surveyed in the Rio Cordon.

run, and cascade channel segments. Reach-average flow depths were derived for use in hydraulic geometry relations from the continuity equation, using discharge measured at the Rio Cordon station, salt-dilution velocities, and the average of cross-section flow widths.

The Rio Cordon field data were also combined with surveyed reach gradients and measured flow velocities to calculate Darcy–Weisbach friction factor (Eq. 1). In addition, to evaluate the prevalence of sub-critical and super-critical flow on a reach-averaged basis, Froude number (*Fr*) was calculated as:

$$Fr = \frac{v}{\sqrt{gd}} = \frac{v}{\sqrt{g\frac{A}{w}}} = \frac{v}{\sqrt{g\left(\frac{Q/v}{w}\right)}}, \quad (7)$$

where d is the reach-averaged flow depth (m).

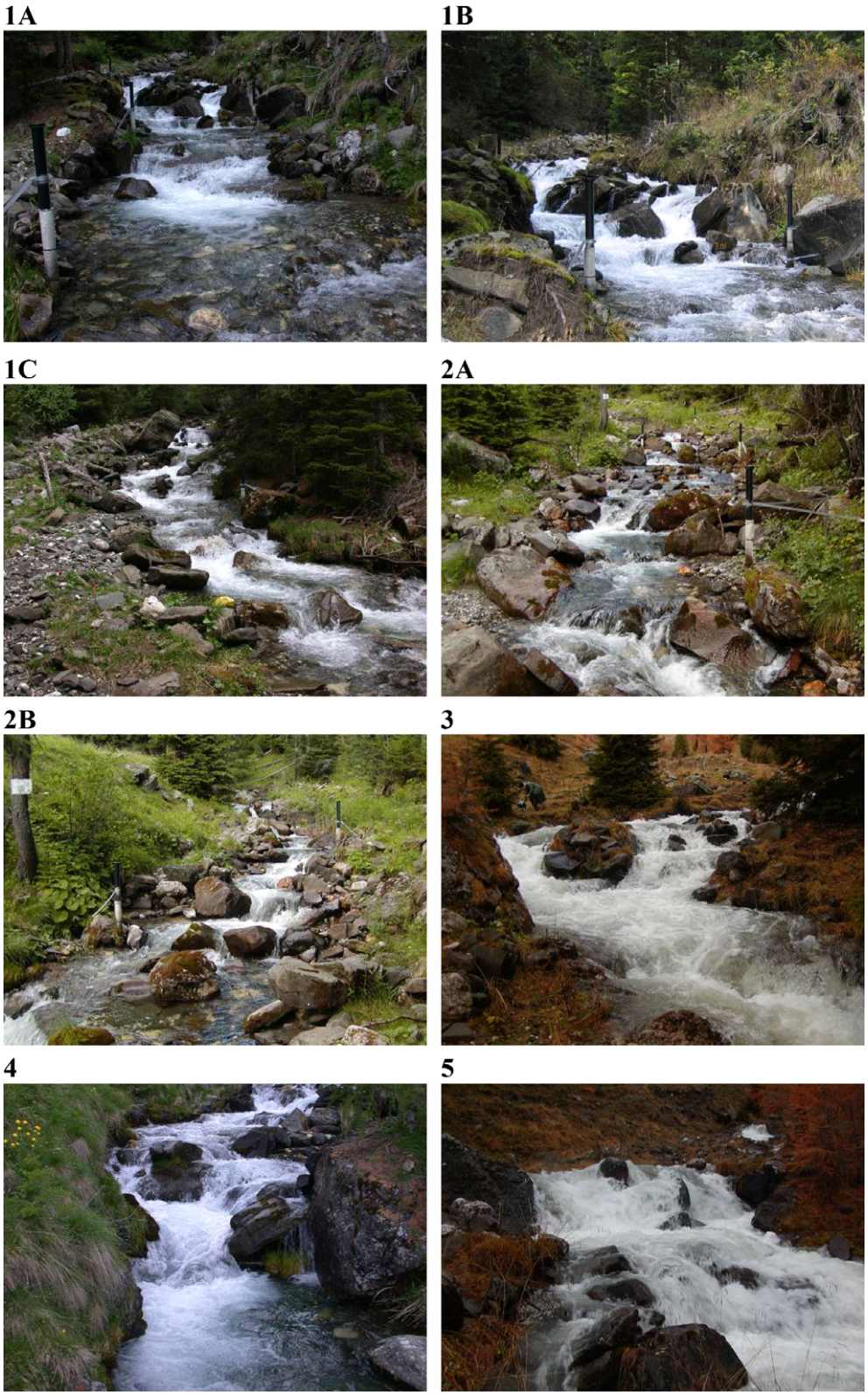

Figure 3 Upstream views of the Rio Cordon reaches. Tumbling flow over steps is prevalent, but pools are often poorly developed, especially in reaches classified as cascades (3 and 5). Several crest gages are visible in the pictures.

Pebble counts by the grid-by-number method were performed in each reach (average sample size > 100) to obtain the surface grain size distribution, using an integrated, reach-average approach (i.e. no separate counts for different channel units; Bunte and Abt, 2001).

Analysis of step-pool hydraulics using combined field datasets

In order to explore factors influencing velocity and flow resistance in step-pool channels, we combined our Rio Cordon data with four other field datasets from step-pool channels, each of which employed salt dilution methods to measure reach-average velocity (Lee and Ferguson, 2002; MacFarlane and Wohl, 2003; Curran and Wohl, 2003; Wohl and Wilcox, 2005). Lee and Ferguson (2002) measured mean velocity along six step-pool reaches ($S = 0.03—0.18$) in the Pennine hills, England, over a range of low to intermediate discharges. MacFarlane and Wohl (2003) and Curran and Wohl (2003) each measured velocity at low flows in 20 step-pool streams ($S = 0.04—0.18$) on the western slope of the Cascade Range, Washington; the Curran and Wohl data focused on LWD-rich streams. Wohl and Wilcox (2005) measured low-flow conditions on 26 step-pool reaches along streams in the South Island of New Zealand ($S = 0.02—0.19$). Two unpublished data points from East St. Louis Creek ($S = 0.11$, Colorado Rocky Mountains, hereafter called ''ESL'') are also included, for a total of $n = 177$ velocity and flow resistance data. Flume data are not considered here in order to focus on the hydraulics of natural step-pool channels.

We used these data to investigate how velocity and flow resistance are affected by several easily measurable channel and hydraulic attributes, including unit discharge ($q = Q/w$), bed roughness (D_c), channel slope (S), and variables describing step-pool geometry. To facilitate analysis over a range of channel sizes and hydraulic conditions, we evaluated velocity in non-dimensional terms. Following Aberle and Smart (2003) and Ferguson (2007), velocity can be non-dimensionalized as follows:

$$v^* = aq^{*b}S^c, \tag{8}$$

where

$$v^* = \frac{v}{\sqrt{gD_c}}, \tag{9}$$

$$q^* = \frac{q}{\sqrt{gD_c^3}}, \tag{10}$$

a is an empirical coefficient and D_c is a roughness parameter. Ferguson (in press) illustrates that the non-dimensional hydraulic geometry relation represented by Eq. (8) can also be derived from a power-law resistance relationship analogous to Eq. (6) (assuming $d \approx R_h$) and applying the continuity equation for discharge.

In order to evaluate controls on and develop equations for dimensionless velocity (v^*) and Darcy—Weisbach friction factor (ff), multiple regression analyses were performed on these dimensionless parameters using the combined field dataset. The software Statistica 6 was used, and the ordinary least squares method was adopted. The following independent variables were included in the analysis: q^*, S, R_h/D_{84}, pool frequency (number of pools per reach length), step height-length ratio (H/L), and relative steepness ($(H/L)/S$, Abrahams et al. 1995). A non-linear multiple regression was carried out for flow velocity data. A logarithmic transformation was applied to ff in order to stabilize variances for the subsequent multiple linear regression analysis.

An initial step in our multiple regression analysis entailed regressing different bed roughness variables (D_{50}, D_{84}, s) from the Rio Cordon (Table 1) against velocity in order to determine the appropriate roughness parameter (D_c) for non-dimensionalizing $v$and q with Eqs. (9) and (10). This analysis used Rio Cordon data only, because data on certain roughness parameters (e.g., standard deviation of the bed profile) were not available for all datasets. The D_{84} showed the highest correlation with flow velocity among the Rio Cordon reaches; we therefore set $D_c = D_{84}$ in Eqs. (9) and (10) for subsequent analysis.

Results

Hydraulics in the rio cordon

Reach-average velocities measured in the Rio Cordon ranged from approximately 0.2 m s^{-1} (Reach 1A, $Q = 0.08$ m^3 s^{-1}) to 1.4 m s^{-1} (Reach 1C, $Q = 1.5$ m^3 s^{-1}). This maximum velocity was higher than the velocity recorded at the highest discharge in our study ($v = 1.1$ m s^{-1} at $Q = 1.86$ m^3 s^{-1}, 80% of Q_{bf}), because this measurement comes from a different reach (1A).

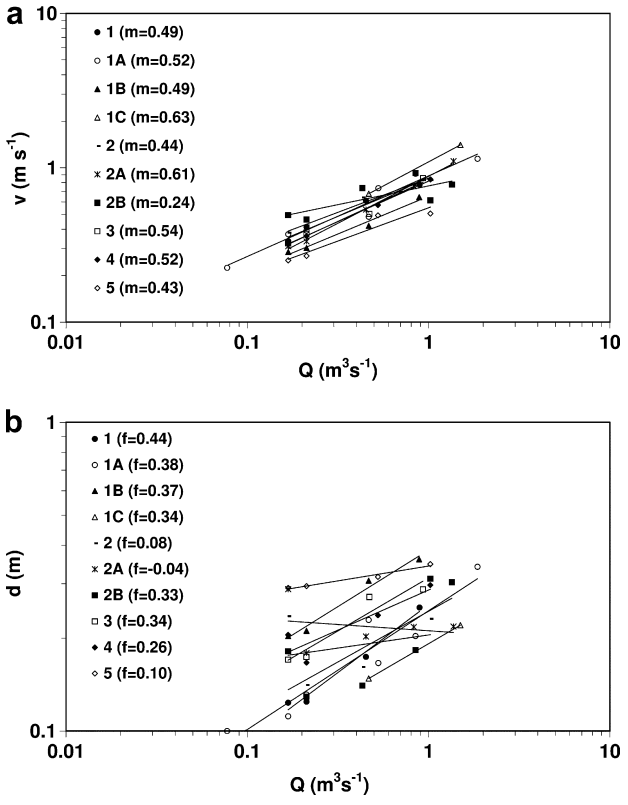

Figure 4 At-a-station hydraulic geometry relations for the study reaches on the Rio Cordon. (a) Reach-averaged velocity v versus discharge Q. (b) Continuity-derived flow depth d versus discharge Q. (c) Reach-averaged channel top width w versus discharge Q. The parenthetical values for m, f, and b represent the slopes of the best-fit power function relations between Q and v, d, and w, respectively and reflect standard notation for hydraulic geometry relations.

The hydraulic geometry analysis indicated that in most reaches, velocity increased more rapidly with discharge than width or depth (Fig. 4). The velocity exponent m ($v = kQ^m$) ranged from 0.24 to 0.63 and averaged 0.48 for all reaches (Fig. 4a). Most reaches had velocity exponents between 0.48 and 0.6, and the exponents for the non-step-pool reaches in the analysis (1A, 3, and 5) were similar to those for step-pool reaches. Patterns of changes in reach-average width and depth with discharge showed more variation among reaches (Figs. 4b and c). Because depths plotted in Fig. 4b are back-calculated using the continuity equation, they incorporate errors in measured velocities, widths, and discharges. The decrease in depth with discharge shown for reach 2A is likely a result of such errors (Fig. 4b).

Changes in flow resistance with discharge are shown for each reach in Fig. 5. The slopes of the ff versus Q regressions in most of the Cordon reaches are between approximately −0.35 and −0.6, indicating that resistance decreases approximately with the square root of discharge. One reach (2B) exhibits a positive relationship between ff and Q, although the relationship is weak and contains considerable scatter. The highest flow resistance values at both low and high discharges were measured in Reach 5 (Fig. 5), a cascade reach featuring the steepest gradient, the coarsest grain size distribution, the largest bed profile roughness (s), and the lowest measured velocities among our study reaches (Table 1, Fig. 4a). The other, lower slope cascade reach (reach 3), shows ff values only slightly higher than the average of the entire dataset. The lowest ff values were measured at Reach 1C, but only two measurements are available. Low flow resistance is evident over a wider discharge range in Reach 1A, the only run among our study reaches, and in Reach 2B, a step-pool segment with a low steepness factor $(H/L)/S$ and a low standard deviation of the bed profile s (Table 1).

On a reach-averaged basis, sub-critical ($Fr < 1$) conditions occurred in all reaches at all discharges, despite visual evidence of locally occurring super-critical flow within these reaches. The only near-critical flow ($Fr = 0.96$) was recorded at the highest dimensionless flow rate (reach 1C, $q^* = 0.52$). All the other Rio Cordon data are characterized by $Fr < 0.8$, even at flows approaching bankfull conditions.

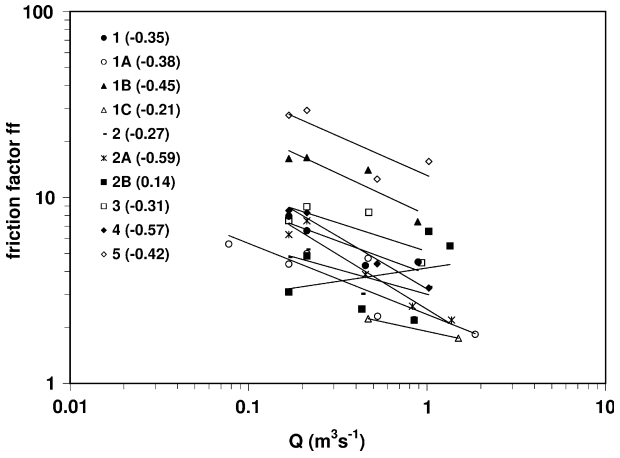

Figure 5 Darcy–Weisbach friction factor ff versus discharge Q for the Rio Cordon channel reaches.

Analysis of combined step-pool field data

Effects of unit discharge, channel slope and bed morphology on velocity

Mean flow velocity and unit water discharge for the combined datasets show a strong and consistent positive relationship (Fig. 6), as would be expected because of the collinearity among these terms. We also evaluated the relationship between v and q in dimensionless terms (Fig. 7), where v and q were non-dimensionalized using D_{84} as the representative roughness parameter (D_c) in Eqs. (9) and (10). The best-fit equation obtained through regression of all the field data ($n = 177$, $R^2 = 0.81$, $p < 0.001$), which results in a dimensionless hydraulic geometry relationship, is:

$$v^* = 0.92q^{*0.66}. \quad (11)$$

Non-dimensionalizing v and q and accounting for bed roughness (i.e., D_{84}) produces improved correlations within each dataset compared to Fig. 6. Table 2 reports the coefficient a and exponent b and R^2 values for each dataset.

Next, we used the step-pool datasets to investigate effects of channel slope on velocity in step-pool channels by applying a non-linear regression (through the ordinary least-squares method) to Eq. (8). For the combined dataset, this results in the following relationship ($n = 177$, $R^2 = 0.81$):

$$v^* = 0.97q^{*0.67}S^{0.01}. \quad (12)$$

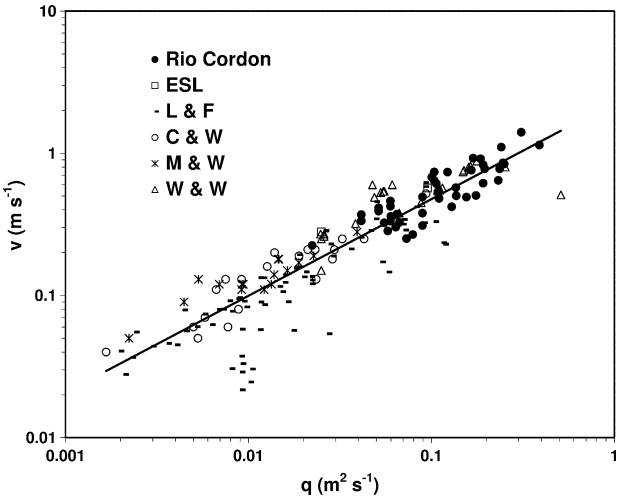

Figure 6 Relationship between mean flow velocity (v) and unit water discharge (q) for datasets from the Rio Cordon, East St. Louis (ESL) Creek, Lee and Ferguson (2002, L & F); MacFarlane and Wohl (2003, M & W); Curran and Wohl (2003, C & W); and Wohl and Wilcox (2005, W & W). Correlation coefficients for individual datasets, ranked from highest to lowest, are as follows: Curran and Wohl (2003), $R^2 = 0.86$; MacFarlane and Wohl (2003), $R^2 = 0.83$; Rio Cordon, $R^2 = 0.74$; Lee and Ferguson (2002), $R^2 = 0.71$; Wohl and Wilcox (2005), $R^2 = 0.61$. The solid line represents the overall best-fit equation ($v = 2.28q^{0.68}$, $R^2 = 0.83$).

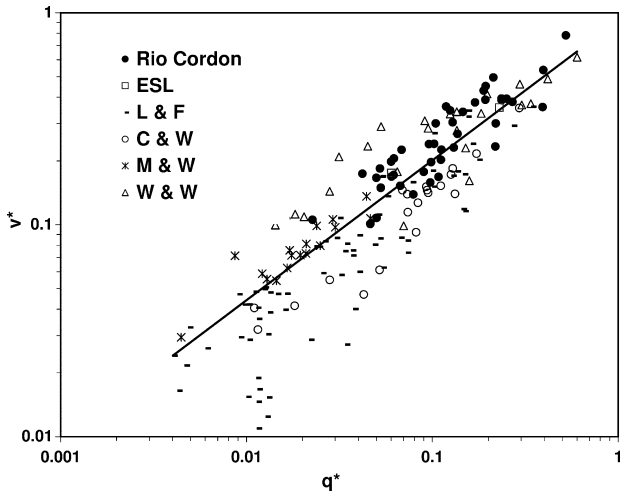

Figure 7 Relationship between dimensionless unit discharge (q^*) and dimensionless velocity (v^*) (see Fig. 6 caption for description of datasets). The solid line represents the best-fit equation (Eq. 11): $v^* = 0.92q^{*0.66}$.

Adding S to the equation for predicting v^* does not increase the variance explained compared to Eq. (11), and the exponent of S is not statistically significant. This suggests that the dimensionless velocity used here is not directly affected by S; although S may indirectly influence velocity through its influence on D_{84}, which is incorporated into v^*. This contrasts with dimensional equations for velocity in which v is related to $S^{0.5}$ (Eq. 1) or, where velocity appears on the right side of the equation as part of unit discharge, as in Eqs. (3) and (4), to $S^{0.2}$.

Examining the datasets separately, however, shows widely varying slope exponents, ranging from −0.47 for the Rio Cordon (i.e., v^* varies approximately inversely with the square root of slope) to 0.26 for Curran and Wohl's (2003) data (Table 2). The unique relationship between v^* and S observed in the Rio Cordon compared to the other channels may reflect the wider discharge range for which flow velocity measurements are available, as well as the morphologic characteristics of the Cordon's reaches. The steepest reaches (Reaches 1B, 3, 5) on the Cordon have considerable roughness from large clasts, step-pool sequences, and/or median bars that likely reduce flow velocity. Moreover, the reach with the lowest slope (reach 1A) can be classified as a run and therefore does not produce spill resistance associated with plunging flow over step-pool sequences. Increases in roughness as gradient increases on the Rio Cordon therefore appear to outweigh gravitational effects on flow velocity. No other standard parameters (i.e. relative roughness, R_h/D_{84} or d/D_{84}) were found to explain significantly this slope-related variation. Indeed, Jarrett (1984) had already observed that channel slope rather than relative submergence seems more efficient in predicting equations for flow resistance in mountain rivers.

By plotting together the empirical equations for each dataset, for different channel slopes and in the range $0.01 < q^* < 1$ (graphs not shown), it can be computed that, overall, Rio Cordon's equation tends to predict relatively higher dimensionless velocities, whereas the equation obtained from the Curran and Wohl (2003) data leads to the lowest velocities. The reasons may be linked to the relatively poor development of pools in the Rio Cordon and to the presence of additional resistance to flow by LWD in the Curran and Wohl streams.

We also investigated how including geometric variables in equations for dimensionless velocity improved predictive ability. This analysis, which included pool frequency (i.e., number of pools per reach length), step height-length ratio H/L, and relative steepness $(H/L)/S$, was performed on all datasets except for that of Lee and Ferguson (2002), for which step geometry data are not available. Pool frequency and H/L did not show significant correlations with v^*. The best result of the non-linear regression is obtained with the steepness factor $(H/L)/S$,leading to the following equation ($n = 107$, $R^2 = 0.83$):

$$v^* = 0.74q^{*0.59}\left(\frac{H/L}{S}\right)^{0.52}, \quad (13)$$

where the coefficients and all the exponents are significant ($p < 0.005$). The total range of variation of $(H/L)/S$ is 0.52—2.22 (with $H/L = 0.03$—0.32). If $(H/L)/S$ is not included in the regression on the same partial ($n = 107$) dataset, the correlation coefficient decreases to 0.80. This suggests that using a parameter describing step-pool geometry may be of only slight advantage for the prediction of flow velocity in steep streams, although as discussed below, step-pool geometry shows a stronger influence on flow resistance. For the same dataset used in Eq. (13), H/L and S are highly correlated ($R^2 = 0.80$), as represented by the quasi-linear relationship $H/L = 1.42S^{1.05}$.

Flow resistance relationships

Flow resistance data from the Rio Cordon and other step-pool channels were also examined to assess relationships

Table 2 Parameters of the best-fit equations relative to v^* (Eqs. (11) and (12)) for each dataset

Dataset	N	Fr	$v^* = aq^{*b}$			$v^* = aq^{*b}S^c$			
			a	b	R^2	a	b	c	R^2
Rio Cordon	44	0.15—0.96	0.97	0.62	0.781	0.35	0.61	−0.47	0.863
L & F (2002)	70	0.01—0.52	0.76	0.68	0.801	0.57	0.65	−0.08	0.809
M & W (2003)	17	0.08—0.29	0.66	0.55	0.833	0.89	0.56	0.09	0.845
C & W (2003)	20	0.05—0.39	0.93	0.81	0.935	1.88	0.87	0.26	0.951
W & W (2005)	24	0.12—0.68	0.71	0.44	0.799	0.46	0.39	−0.11	0.803

The range of Froude numbers associated with each dataset is also reported.

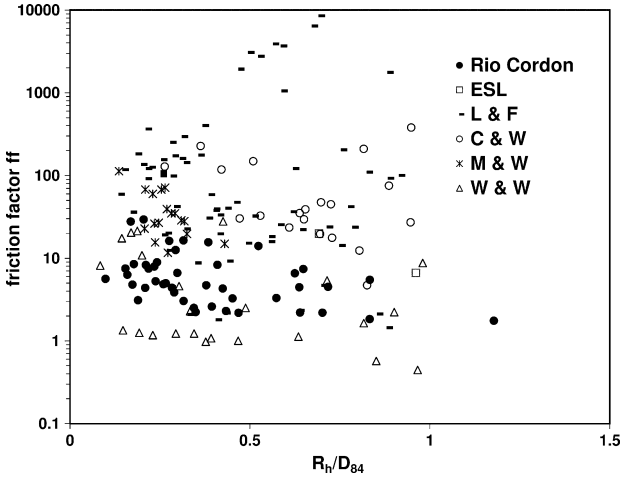

Figure 8 Semi-logarithmic plot of *ff* versus the submergence ratio R_h/D_{84} for all the datasets. A common trend is not present, but each individual dataset (apart from Lee and Ferguson, 2002) shows a moderate negative correlation between the two parameters.

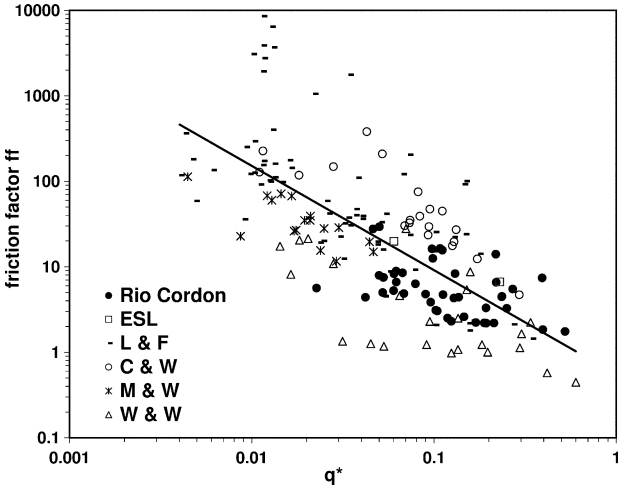

Figure 9 Relationship between resistance factor *ff* and dimensionless unit discharge q^*. The solid line represents the best-fit equation (Eq. 14): $ff = 0.55q^{*-1.22}$.

with factors including relative submergence (R_h/D_{84}), unit discharge, slope, and step geometry. Flow resistance equations for lower-gradient channels often relate *ff* to R_h/D_{84}, including approaches based on the logarithmic law of the wall (e.g., Keulegan, 1938; Parker and Peterson, 1980) and empirical power-law approaches (e.g., Bathurst, 2002). In Fig. 8, the resistance factor is plotted against relative submergence for all the available datasets. The conditions are of very large relative roughness, where $0.1 < R_h/D_{84} < 1.2$, and under these conditions approaches based on the law of the wall are no longer valid (Katul et al., 2002). In fact, for the combined data, no overall relationship between *ff* and R_h/D_{84} is evident, and very large variations in *ff* are evident for similar submergence ratios, even within single datasets (Fig. 8). Correlations between *ff* and other bed roughness variables (i.e. D_{90}, *s*, where these variables are available) were also examined and are similarly poor. Despite considerable scatter, most of the individual datasets exhibit the expected negative relationship between *ff* and R_h/D_{84} (Fig. 8).

We also examined the relationship between flow resistance and dimensionless unit discharge q^* (Fig. 9). The relationship can be expressed by the following equation, obtained by linear regression on the log-transformed data ($n = 177$, $R^2 = 0.51$):

$$ff = 0.55q^{*-1.22}. \quad (14)$$

Table 3 reports the coefficients of the best-fit equations for each individual dataset. Within the overall pattern of a negative relationship between *ff* and q^*, some of the individual datasets exhibit distinct characteristics. Curran and Wohl (2003) recorded higher resistance factors at comparable dimensionless unit discharges compared to the broader dataset (Fig. 9), perhaps as a result of the higher flow resistance induced by LWD in Curran and Wohl's streams. Wohl and Wilcox's (2005) New Zealand data exhibit low resistance factors (Fig. 9), potentially because those streams have low channel gradients relative to other streams in the combined dataset and lack LWD. The other datasets are approximately equally distributed across the best-fit curve.

In order to quantify the influence of channel slope on flow resistance, a multiple linear regression on log-transformed data was performed ($n = 177$; $R^2 = 0.61$):

$$ff = 10.47q^{*-1.13}S^{1.12}, \quad (15)$$

with all the coefficients significant at $p < 0.001$. Channel slope is therefore found to have a strong — slightly more than linear — influence on flow resistance, as would be expected because *S* is used in the calculation of *ff* (Eq. 1). Collinearity is thus present between the two variables, as well as between *ff* and q^*. Large variation occurs among the different streams, however, as evident from the comparison of different exponents in Table 3. The Rio Cordon shows the largest increase in R^2 by incorporating *S* in equations for *ff* (i.e., using an equation of the form of (15) rather than (14)) (Table 3). This suggests strong influences of *S* on *ff* in the Rio Cordon compared to other datasets examined here, an effect related to the correlation between v^* and *S* for the Rio Cordon discussed above.

We also examined the effect of including $(H/L)/S$ in predictive equations for *ff*, as we did for velocity (Eq. 13). The following equation was determined using all data except for those of Lee and Ferguson (2002) ($n = 107$; $R^2 = 0.51$, all parameters significant at $p < 0.05$):

$$ff = 1.90q^{*-0.58}\left(\frac{H/L}{S}\right)^{-0.31}. \quad (16)$$

The correlation for Eq. (16) compares favourably with the regression omitting $(H/L)/S$ for the same reduced dataset, for which $R^2 = 0.42$, but is lower than if *S* is used instead, as in (15) ($R^2 = 0.54$). Inserting H/L in the regression produces the following ($n = 107$; $R^2 = 0.46$, all parameters significant at $p < 0.01$):

$$ff = 2.98q^{*-0.63}\left(\frac{H}{L}\right)^{0.20}. \quad (17)$$

Although the R^2 is lower than Eq. (16), the collinearity between *ff* and *S* is eliminated here. The positive value of

Table 3 Parameters of the best-fit equations for Darcy–Weisbach friction factor (ff) (Eqs. (14) and (15)) for each dataset

Dataset	N	$ff = Aq^{*B}$			$ff = Aq^{*B}S^{C}$			
		A	B	R^2	A	B	C	R^2
Rio Cordon	44	1.90	−0.47	0.215	87.10	−0.50	1.83	0.783
L & F (2002)	70	0.79	−1.26	0.458	123.03	−0.98	1.63	0.692
M & W (2003)	17	1.38	−0.79	0.52	20.89	−0.72	0.99	0.733
C & W (2003)	20	2.82	−1.04	0.676	7.94	−1.08	0.50	0.694
W & W (2005)	24	0.45	−0.77	0.465	389.04	0.05	1.67	0.637

the H/L exponent indicates that greater relative step heights produce higher flow resistance, whereas the analysis above found no relationship between H/L and v^*. The positive relationship between flow resistance and H/L in Eq. (17) agrees with the laboratory findings of Maxwell and Papanicolaou (2001) and Wilcox and Wohl (2006b).

Comparison with flume-derived equations

We used the Rio Cordon dataset (n = 44) to evaluate the predictive performance of equations for velocity and flow resistance based on laboratory experiments (Eqs. (2)–(5)) and mixed laboratory-field data (Eq. 6). Some variables required by those equations were not readily available for all the other field datasets. We calculated the average relative error, e = |predicted values − observed values|/observed values), to assess differences between predicted and measured variables.

Predicted flow velocities in the Rio Cordon based on Eqs. (3) and (4) have average errors of 24% and 22%, respectively, compared to observed velocities. Eqs. (3) and (4) tend to underestimate velocities, especially those higher than 1 m s^{-1} (Fig. 10a). Much larger errors are apparent when comparing predicted and observed flow resistance in terms of $(8/ff)^{0.5}$ (Fig. 10b). Average relative errors for Eqs. (2), (5), and (6) are 58%, 98%, and 62%, respectively. Published equations tended to overestimate flow resistance, especially Maxwell and Papanicolaou's Eq. (5) (Fig. 10b), mirroring the underestimation of velocity by these equations. The relatively poor development of step-pool morphology in the Rio Cordon may result in lower flow resistance than in other step-pool channels, resulting in overestimation of flow resistance in the Rio Cordon when generic equations are applied.

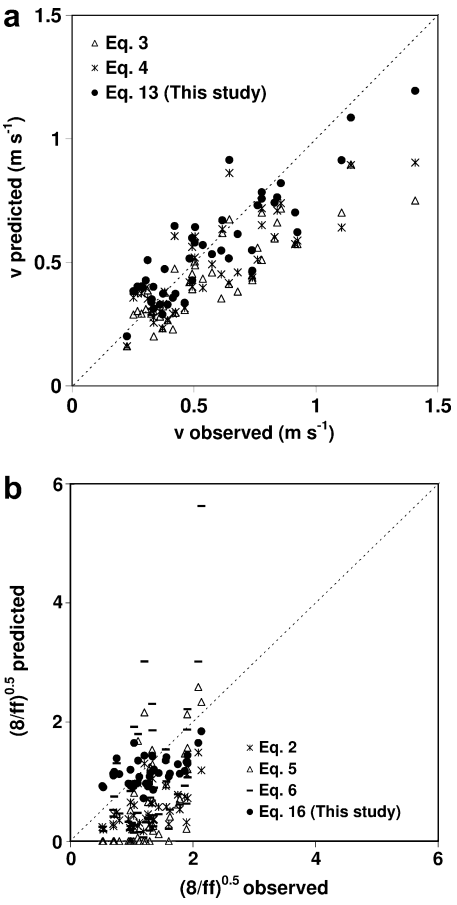

Figure 10 Observed values of flow velocities (a) and resistance (b) in the Rio Cordon against the values predicted by Rickenmann (1990, Eq. (4)), Aberle and Smart (Eqs. (2) and (3)), Maxwell and Papanicolaou (2001, Eq. (5)), Lee and Ferguson (Eq. 6), and by the field-based equations (Eqs. (13) and (16)). Several points relative to (5) have been assigned to zero instead of their predicted negative values. Dashed lines illustrate 1:1 relationships between observed and predicted values.

Discussion

Controls on velocity and flow resistance

Our analysis found that dimensionless unit discharge was the most important independent variable for explaining dimensionless velocity for a large dataset from step-pool channels. We also found that when channel slope was added to regression equations relating dimensionless velocity and unit discharge for the combined step-pool dataset, the effect of channel slope on dimensionless velocity was limited (as earlier observed by Matakiewicks, in Indri, 1942). This contrasts with laboratory equations for v such as Eqs. (3) and (4), analogous in dimensional terms to Eq. (12), in which velocity is related to $S^{0.2}$. For the Rio Cordon, however, dimensionless velocity showed an inverse correlation with bed gradient, perhaps reflecting the effect of increasingly irregular and hydraulically rough bed morphology with increasing slope.

For the combined field dataset, flow resistance does increase with channel slope, as suggested by Eq. (1) and as observed in mountain rivers by Jarrett (1984). This effect may

be especially relevant to strong macro-roughness conditions ($R_h/D_{84} < 1.8$; Bathurst, 2002), although our results also indicate that, in contrast to lower-gradient channels, submergence ratios such as R_h/D_{84} are poor predictors of flow resistance in steep mountain rivers. Our finding that dimensionless unit discharge performs better than R_h/D_{84} for flow resistance estimation may be analogous to findings that the critical discharge approach is preferable to the use of boundary shear stress for estimating incipient sediment motion in steep streams (Bathurst et al., 1987; Ferguson, 1994; Lenzi et al., 2006b).

Our analysis treats flow resistance in terms of total resistance, such that resistance is not partitioned into distinct components such as grain and form roughness. Recent field and flume studies have suggested that resistance partitioning is important in step-pool channels, however, because resistance in these channels is dominated by spill resistance, which is generated by tumbling flow over step-pool bedforms, and, where LWD is present, by debris resistance (Curran and Wohl, 2003; MacFarlane and Wohl, 2003; Wilcox and Wohl, 2006b; Wilcox et al., 2006). Standard approaches to predicting flow resistance in lower-gradient channels, such as Keulegan-type equations relating friction factor to submergence ratios such as R_h/D_{84}, often assume that resistance is dominated by grain roughness, which may explain the poor performance of such methods in predicting flow resistance in steep mountain rivers with substantial form and spill roughness (Fig. 8). Quantifying distinct components of flow resistance in steep channels presents a substantial challenge, however.

Calculation of flow resistance in steep channels can be highly sensitive to errors in the measurement of channel geometry. Hydraulic radius and flow depth can be highly variable along reaches of steep channels that alternate between step, pool, and transition units, and methods used to calculate these variables can strongly influence results. For example, in the Rio Cordon, flow depths calculated from cross-section surveys range from 0.3 to 2 times the reach-averaged depth back-calculated based on flow continuity. Friction factor values calculated using reach-averaged depths are approximately 20% larger than *ff* values computed from cross-section measurements of R_h.

Our Rio Cordon data may also be affected by lack of precision in velocity measurements, because the conductivity probes we used for salt-dilution measurements recorded at only 5-s intervals. Sensitivity analysis of the effect of this measurement interval on mean velocity estimates indicated potential errors ranging from 2% to 33%, depending on both reach length and discharge (because travel time decreases with discharge), and averaging 10%. Such errors are propagated to friction factor values (Eq. 1). Errors associated to the estimation of the hydraulic radius or hydraulic depth can be expected to be of the same order, as well as those associated to the determination of the representative bed roughness (i.e. typically the D_{84}).

Hydraulic geometry

Table 4 lists values of at-a-station hydraulic geometry exponents for velocity, depth, and width from the Rio Cordon and various published studies; exponents for the individual Cordon reaches are also shown in Fig. 4. The average of the velocity exponents along the Cordon (0.49) is within the range of values for pool-riffle and step-pool channels but is substantially greater than Leopold and Maddock's (1953) average value for large rivers (0.34). The average of the Cordon's depth exponents is slightly lower than those reported for pool-riffle channels but is within the range reported by Bathurst (1993) and Lee and Ferguson (2002) for step-pool channels. In contrast, the average width exponent from the Cordon reaches is substantially higher than other values in Table 4, with the exception of Leopold and Maddock's (1953) width exponent for large rivers. All of the hydraulic geometry relations for the Cordon show considerable scatter, but the variability among the width and depth exponents is especially large (Fig. 4). As noted above, flow depths in our hydraulic geometry analysis are back-calculated using the continuity equation; therefore, errors in measured velocities, widths, and discharges likely

Table 4 Values of at-a-station hydraulic geometry exponents from various studies

Source	*m* (velocity)[a]	*f* (depth)[a]	*b* (width)[a]
Leopold and Maddock (1953)[b]	0.34	0.40	0.26
Richards (1973)	0.61 (0.14), 0.49—0.78	0.31 (0.16), 0.12—0.48	—
Knighton (1975)[c]	0.48 (0.15), 0.24—0.71	0.40 (0.10), 0.26—0.63	0.11 (0.12), 0.01—0.33
Knighton (1979)[d]	0.42, <0.1—0.8	0.43, <0.1—0.8	0.16, <0.1—0.6
Wohl[e]	0.54 (0.08), 0.43—0.62	—	—
Bathurst (1993)[f]	0.42—0.70	0.19—0.48	0.08—0.14
Lee and Ferguson (2002)[g]	0.51—0.84	0.19—0.36	0.11—0.21
Rio Cordon	0.49 (0.11), 0.24—0.63	[h]0.29 (0.13), [h]0.08—0.44	0.25 (0.18), 0.03—0.47

[a] Exponent values shown include mean and, where available, standard deviation (in parentheses) and range.
[b] Data from large rivers in the Great Plains and southwestern US.
[c] Data from two pool-riffle channels in the UK.
[d] Mean values of data from 206 cross-sections and various authors.
[e] Unpublished data from a pool-riffle channel segment.
[f] Collection of previous studies from boulder and steep pool/fall streams.
[g] Data from step-pool channels in the UK.
[h] A negative exponent found for one reach is not included in this summary.

contribute to the large amount of scatter in the depth-discharge relation (Fig. 4b).

The similarity in velocity exponents among pool-riffle and step-pool channels (Table 4) is surprising given the very different sources of roughness in these channel types. Both Kellerhals (1973) and Bathurst (1993) suggest that steeper channels with tumbling flow and smaller widths should have higher m values than lower-gradient channels (reviewed by Aberle and Smart, 2003). Differences may be obscured by our use of reach-average hydraulic values in the Rio Cordon analysis instead of data from single cross-sections, as in traditional at-a-station hydraulic geometry analysis. Whereas our analysis showed no clear differences in reach-average hydraulic geometry between cascade and step-pool reaches, Richards (1973) found that hydraulic geometry relations differed among morphologic units within a pool-riffle channel. Higher values of the velocity exponent were observed in pools (average $m = 0.74$), where slope increases rapidly with discharge, than in riffles (average $m = 0.54$). Richards (1973) proposed that non-linear variations in roughness give rise to similar non-linear changes of depth and velocity with discharge at a cross-section or along a short segment of channel. Knighton (1975) also found highly variable rates of at-a-station change for pool-riffle channels in England, which he correlated with both cross-sectional shape and the source of roughness. Unless width increased rapidly with discharge, velocity tended to increase faster than depth. Velocity varied inversely with resistance, which decreased most rapidly where grain roughness was the main resistance element (Knighton, 1975).

We also compared changes in Darcy–Weisbach friction factor with discharge from the Rio Cordon against published values. Richards (1973) reported friction factor exponents ranging from −1.37 to 0.64 for a pool-riffle channel. Richards found that a rapid increase in velocity generally occurs in association with a highly negative value of the friction exponent, except when slope increases rapidly with discharge (e.g. a pool location). As noted above, in the Rio Cordon flow resistance decreases approximately proportionally to the square root of discharge, but a clear trend is not apparent in the relationship between the exponents for ff and v.

Conclusion

Steep mountain streams pose serious problems to the application of traditional flow resistance concepts and models, such as the use of the Darcy–Weisbach friction factor or any other roughness coefficient. Estimates of velocity and flow resistance in step-pool channels are highly sensitive to measurement errors and the choice of representative cross-sections, especially given the extreme irregularity of both thalweg and stream banks in step-pool channels. Our analysis suggests that when the discharge is known or assumed and flow velocity is the prediction target – as in many hydrological and hydro-ecological applications – direct estimation of mean flow velocity based on unit water discharge is preferable to using predictive equations for flow resistance as a means of estimating velocity (Rickenmann, 1990; Aberle and Smart, 2003; D'Agostino, 2005; Ferguson, 2007). Indeed, Ferguson (2007) found that the unit discharge method is subject to smaller prediction errors over a wide range of flows ($0.002 < q^* < 100$), allowing for a change in the exponents in Eq. (8) at the transition ($q^* \approx 1$) between relatively shallow and deep flows.

As discussed by Bathurst (2002), flow resistance relationships for mountain rivers are commonly derived by fitting different ensembles of data from different sites, i.e. the between-sites approach, thus limiting full understanding of the physical processes behind the outcome of a certain equation form with its coefficients and exponents. The at-a-site approach (Bathurst, 2002) may provide greater insight into how flow resistance is affected by relative submergence, channel slope, and by other potential variables. When flow velocity and/or flow resistance in steep (>5%), step-pool streams is to be analyzed and modeled to provide predictive equations for engineers and stream managers, however, the paucity of field data limits the ability to derive statistically sound at-a-station analysis.

The between-site analysis combining the Rio Cordon data and other hydraulics data from step-pool streams enables us to obtain field-based dimensionless equations that may be more reliable over a wider range of flow conditions than previously available flume-derived formulas, given the challenges of adequately representing the morphologic and hydraulic complexity of step-pool channels in a laboratory. Substantial differences still emerge among the step-pool channels analyzed here as a result of unique characteristics of bed morphology both at the reach (e.g. bedform steepness) and unit (e.g. three-dimensional pool shape, step irregularity) scale. Fully incorporating such morphologic complexities into predictive equations is impractical, however, and an approach involving only easily determinable macro-variables is preferable.

Additional field measurements with an ''at-a-site'' approach are needed in order to broaden the findings from the Rio Cordon on step-pool hydraulic geometry. Complementing such efforts with further between-sites analysis will improve understanding of step-pool hydraulics over a range of conditions and improve our ability to predict velocity and flow resistance in these channels. Field measurements at high flows (at and above bankfull stage) are especially lacking, strongly limiting the accuracy of the derived equations for high-flow conditions.

Acknowledgements

Funding for this research was provided by the ''Epic Force'' Project EC Contract No. INCO-CT-2004-510735, from the MIUR Project PRIN 2004 No. 2004072251 ''Opere di riqualificazione ambientale dei corsi d'acqua: dalla scala di laboratorio a quella di campo'', and from the University of Padova Project ''Valutazione della pericolosità connessa a colate detritiche e trasporto solido su conoidi alpini''. Participation by Wohl and Wilcox was supported by NSF grant INT-0216951 and by a National Research Council Research Associateship Award to Wilcox. Our thanks to Prof. Robert Ferguson for having kindly provided his data, for an advance view of his paper, and for a thorough, very helpful pre-review of the manuscript. The reviewers of the manuscript

are thanked for their comments that substantially improved the paper. The manuscript also benefited from reviews of an earlier version by Gregory Pasternack, John Jansen, and two anonymous reviewers.

References

Aberle, J., Smart, G., 2003. The influence of roughness structure on flow resistance on steep slopes. J. Hydraul. Res. 41 (3), 259–269.

Abrahams, A.D., Li, G., Atkinson, J.F., 1995. Step-pool streams: adjustment to maximum flow resistance. Water Resourc. Res. 31 (10), 2593–2602.

Bathurst, J.C., 1985. Flow resistance estimation in mountain rivers. J. Hydraul. Eng.-ASCE 111, 625–643.

Bathurst, J.C., 1993. Flow resistance through the channel network. In: Beven, K., Kirkby, M.J. (Eds.), Channel Network Hydrology. Wiley, Chichester, pp. 69–98.

Bathurst, J.C., 2002. At-a-site variation and minimum flow resistance for mountain rivers. J. Hydrol. 269, 11–26.

Bathurst, J.C., Graf, W.H., Cao, H.H., 1987. Bed load discharge equations for steep mountain rivers. In: Thorne, C.R., Bathurst, J.C., Hey, R.D. (Eds.), Sediment Transport in Gravel-Bed Rivers. Wiley, Chichester, pp. 453–491.

Bunte, K., Abt, S.R., 2001. Sampling surface and subsurface particle-size distributions in wadable gravel- and cobble-bed streams for analysis in sediment transport, hydraulics, and streambed monitoring. Report RMRS-GTR-74, USDA Forest Service, 409 pp.

Calkins, D., Dunne, T., 1970. A salt tracing method for measuring channel velocities in small mountain streams. J. Hydrol. 11, 379–392.

Chin, A., Wohl, E.E., 2005. Toward a theory for step pools in stream channels. Progr. Phys. Geogr. 29 (3), 275–296.

Comiti, F., Lenzi, M.A., 2006. Dimensions of standing waves at steps in mountain rivers. Water Resourc. Res. 42, W03411. doi:10.1029/2004WR00389.

Comiti, F., Andreoli, A., Lenzi, M.A., 2005. Morphological effects of local scouring in step-pool streams. Earth Surf. Process. Landforms 30 (12), 1567–1581.

Comiti, F., Andreoli, A., Lenzi, M.A., Mao, L., 2006. Spatial density and characteristics of woody debris in five mountain rivers of the Dolomites (Italian Alps). Geomorphology 78, 44–63.

Curran, J.C., Wilcock, P.R., 2005. Characteristic dimensions of the step-pool bed configuration: an experimental study. Water Resourc. Res. 41, W02030. doi:10.1029/2004WR00356.

Curran, J.H., Wohl, E.E., 2003. Large woody debris and flow resistance in step-pool channels, Cascade Range, Washington. Geomorphology 51 (1–3), 141–157.

D'Agostino, V., 2004. Sull'affidabilità delle misure di portata nei torrenti montani con il metodo della diluizione salina. In: Proceedings of the 29th Italian Congress of Hydraulics and Hydraulic Structures, Trento, Italy, September 7–10, pp. 1005–1012.

D'Agostino, V., 2005. Velocità media della corrente in torrenti fortemente scabri. In: Proceedings of the Italian Congress AIIA2005, Catania, Italy, June, pp. 27–30.

Egashira, S., Ashida, K., 1991. Flow resistance and sediment transportation in streams with step-pool bed morphology. In: Armanini, A., Di Silvio, G. (Eds.), Fluvial Hydraulics of Mountain Regions. Springer-Verlag, pp. 45–58.

Elder, K., Kattelmann, R., Ferguson, R., 1991. Refinements in dilution gauging for mountain streams. IAHS Publ. 193, 247–254.

Ferguson, R.I., 1986. Hydraulics and hydraulic geometry. Progr. Phys. Geogr. 10, 1–31.

Ferguson, R.I., 1994. Critical discharge for entrainment of poorly sorted gravel. Earth Surf. Process. Landforms 19, 179–186.

Ferguson, R.I., 2007. Flow resistance equations for gravel- and boulder-bed streams. Water Resour. Res., doi:10.1029/2006WR005422.

Hardy, T., Panja, P., Matthias, D., 2005. WinXSPro User's manual, version 3.0. General Technical Report RMRS-GTR-147, Rocky Mountain Research Station, U.S. Forest Service, USDA, p. 104.

Indri, E., 1942. Misure sulla velocità dell'acqua in alvei a forte scabrezza. L'Acqua 20 (9), 113–121.

Jarrett, R.D., 1984. Hydraulics of high-gradient streams. J. Hydraul. Eng.-ASCE 110 (11), 1519–1539.

Judd, H.E., Peterson, D.F., 1969. Hydraulics of large bed element channels. Report PRWG 17-6,Utah Water Research Laboratory, 85 pp.

Katul, G., Wiberg, P., Albertson, J., Hornberger, G., 2002. A mixing layer theory for flow resistance in shallow streams. Water Resourc. Res. 38 (11), 1250. doi:10.1029/2001WR00081.

Kellerhals, R., 1973. Hydraulic performance of mountain streams. In: Proceedings of the 15th Congress of the IAHR, Istanbul, vol. 1, pp. 467–473.

Keulegan, G.H., 1938. Laws of turbulent flow in open channels. J. Natl. Bureau Stand. 21, 707–741.

Knighton, A.D., 1975. Variations in at-a-station hydraulic geometry. Am. J. Sci. 275, 186–218.

Knighton, A.D., 1979. Comments on log-quadratic relations in hydraulic geometry. Earth Surf. Process. 4, 205–209.

Lee, A.J., Ferguson, R.I., 2002. Velocity and flow resistance in step-pool streams. Geomorphology 46 (1–2), 59–71.

Lenzi, MA., 2001. Step-pool evolution in the Rio Cordon, Northeastern Italy. Earth Surf. Process. Landforms 26, 991–1008.

Lenzi, M.A., 2004. Displacement and transport of marked pebbles, cobbles and boulders during floods in a steep mountain stream. Hydrol. Process. 18, 1899–1914.

Lenzi, M.A., D'Agostino, V., Billi, P., 1999. Bedload transport in the instrumented catchment of the Rio Cordon: Part I. Analysis of bedload records, conditions and threshold of bedload entrainment. Catena 36 (3), 171–190.

Lenzi, M.A., Mao, L., Comiti, F., 2003. Interannual variation of sediment yield in an alpine catchment. Hydrol. Sci. J. 48 (6), 899–915.

Lenzi, M.A., Mao, L., Comiti, F., 2004. Magnitude-frequency analysis of bed load data in an Alpine boulder bed stream. Water Resourc. Res. 40, W07201. doi:10.1029/2003WR00296.

Lenzi, M.A., Mao, L., Comiti, F., 2006a. Effective discharge for sediment transport in a mountain river: computational approaches and geomorphic effectiveness. J. Hydrol. 326, 257–276.

Lenzi, M.A., Mao, L., Comiti, F., 2006b. When does bedload transport begin in steep boulder-bed streams? Hydrol. Process. 20, 3517–3533.

Leopold, L.B., Maddock, T., 1953. The hydraulic geometry of stream channels and some physiographic implications. U.S. Geological Survey Professional Paper 252, 56 pp.

MacFarlane, W.A., Wohl, E.E., 2003. Influence of step composition on step geometry and flow resistance in step-pool streams of the Washington Cascades. Water Resourc. Res. 39 (2), W1037. doi:10.1029/2001WR00123.

Mao, L., 2004. Analisi comparativa del trasporto solido di corsi torrentizi in diversi ambiti geografici. Ph.D. Thesis, University of Padova, 307 pp.

Mao, L., Lenzi, M.A, 2007. Sediment mobility and bedload transport conditions in an alpine stream. Hydrological Processes, published online.

Marcus, W.A., Roberts, K., Harvey, L., Tackman, G., 1992. An evaluation of methods for estimating Mannings's n in small mountain streams. Mount. Res. Develop. 12 (3), 227–239.

Maxwell, A.R., Papanicolaou, A.N., 2001. Step-pool morphology in high-gradient streams. Int. J. Sediment. Res. 16, 380–390.

Millar, R.G., 1999. Grain and form resistance in gravel-bed rivers. J. Hydraul. Res. 37 (3), 303—312.

Montgomery, R.D., Buffington, J.M., 1997. Channel-reach morphology in mountain drainage basin. Geol. Soc. Am. Bull. 109 (5), 596—611.

Parker, G., Peterson, A.W., 1980. Bar resistance of gravel-bed streams. J Hydraul. Eng.-ASCE 106, 1559—1573.

Peterson, D.F., Mohanty, P.K., 1960. Flume studies of flow in steep, rough channels. J. Hydraul. Div.-ASCE 86, 55—76.

Richards, K.S., 1973. Hydraulic geometry and channel roughness — a non-linear system. Am. J. Sci. 273, 877—896.

Rickenmann, D., 1990. Bedload transport capacity of slurry flows at steep slopes. Mitt. der Versuchsanstalt für Wasserbau, Hydrologie und Glaziologie, ETH Zürich, Nr. 103.

Rickenmann, D., 1991. Hyperconcentrated flow and sediment transport at steep slopes. J. Hydraul. Eng.-ASCE 117 (11), 1419—1439.

Thompson, S.M., Campbell, P.L., 1979. Hydraulics of a large channel paved with boulders. J. Hydraul. Res. 17, 341—354.

Valle, B., Pasternack, G., 2006. Submerged and unsubmerged natural hydraulic jumps in a bedrock step-pool mountain channel. Geomorphology 82 (1—2), 146—159.

Wilcox, A., Wohl, E.E., 2006a. Three-dimensional hydraulics in a step-pool channel. Geomorphology 83 (3—4), 215—231.

Wilcox, A., Wohl, E.E., 2006b. Flow resistance dynamics in step-pool channels: 1. Large woody debris and controls on total resistance. Water Resourc. Res. 42, W05418. doi:10.1029/2005WR00427.

Wilcox, A., Comiti, F., Wohl, E.E., 2006. Local-scale hydraulics and morphology in a steep channel, Italian Dolomites. Geophysical Research Abstracts, Vol. 8, 05239, European Geosciences Union.

Wilcox, A., Nelson, J.M., Wohl, E.E., 2006. Flow resistance dynamics in step-pool channels: 2. Partitioning between grain, spill, and woody debris resistance. Water Resourc. Res. 42, W05419. doi:10.1029/2005WR00427.

Wohl, E.E., 2000. Mountain Rivers. Water Resource Monograph 14, Washington, DC, USA, p. 320.

Wohl, E.E., Thompson, D.M., 2000. Velocity characteristics along a small step-pool channel. Earth Surf. Process. Landforms 25, 353—367.

Wohl, E.E., Wilcox, A., 2005. Channel geometry of mountain streams in New Zealand. J. Hydrology 300 (1—4), 252—266. doi:10.1016/j.jhydrol.2004.06.006.